Thermal characterization of a R134A two-phase flashing jet

Yildiz D[1]., Rambaud P[1]., Van Beeck J.P.J.A.[1], Buchlin J-M.[1]

1. Von Karman Institute for Fluid Dynamics, Chaussée de Waterloo 72, 1640 Rhode-Saint-Genése, Belgium

This article explains the temperature evolution of a R134-A flashing jet originated from a diaphragm type orifice without flashing before this orifice. Understanding of the flashing phenomena is necessary for the risk assessment of industrial environments and/or for injection technology studies. In the present case, a global temperature measurement is done with intrusive and non-intrusive techniques. The study includes the effect of different orifice diameters on the axial temperature evolution of the flashing jet and their comparisons with a simple analytical model.

1. Introduction

Liquid flashing phenomena holds an interest in many areas of science and engineering. As examples one can mention: a) the accidental release of flammable and toxic pressure-liquefied gases in chemical and nuclear industry; the failure of a vessel or pipe in the form of a small hole results in the formation of a two-phase jet containing a mixture of liquid droplets and vapour, b) fuel atomisation for improvement of fuel injector technology, c) flashing mechanism occurrence in expansion devices of refrigerator cycles etc. The present work focuses on the thermal change in case of a sudden release of pressurized liquefied R134-A that forms a jet after the release.

1.1. Motivation

Violent boiling and aerodynamic fragmentation control the two-phase behaviour of flashing flows. The initial, flashing stage of the jet, where the system is furthest from equilibrium is least understood. To investigate theoretically these source processes, knowledge of accurate and reliable data such as distribution of droplet size, velocity and temperature is mandatory. These models are needed in design and safety assessment. The authors performed preliminary studies for the understanding of droplet size, velocity distributions and temperature evolutions using laser based and intrusive techniques [1&2].

1.2. Description of flashing phenomena

The flashing phenomenon occurs when a liquid is out of thermodynamic equilibrium (see [3,4,5,6,7] for detailed review). Different scenarios may lead to this non-equilibrium. In the first one, a liquid in equilibrium is heated to a higher temperature while its pressure is maintained constant. In the second case, the liquid is depressurized rapidly keeping its initial temperature constant, so that, because of thermal inertia, the internal temperature finds itself above the saturation temperature in the final condition. In the present study, the second scenario is chosen.

Under carefully controlled conditions (pure substance, perfectly clean and smooth vessel, no physical disturbances and slow and almost reversible process) it is possible for a liquid to be maintained in a meta-stable state. However, under most practical circumstances, the ideal conditions cannot be met and the meta-stable liquid will return violently to its equilibrium condition through evaporation (i.e. consuming its superheat as latent heat). As stated by Owen and Jalil [8], if the superheat within the depressurized liquid can be conducted to the interface, the latent heat will be released through surface evaporation. If, however, the heat cannot be conducted at a sufficiently high rate, evaporation will occur within the liquid through bubble growth. This process can be extremely sudden and explosive. Because a maximum surface exchange is crucial for evaporation, the jet will disintegrate into small droplets. Equilibrium will be reached when partial vapour pressure at the interface equals that far way from the droplets (this will never be reached when fresh air is entrained continuously).

1.3. Layout of the paper

The main objective of the present work is to assess the temperature evolution of the two-phase flashing R134-A jet, using intrusive and non-intrusive techniques and compare it to a macroscopic modelling approach. Section 2 will give a detailed description of the macroscopic approach method used for the rapid evaporation of a droplet of R134-A after the jet break-up. Section 3 will give description of the experimental set-up and measurement campaigns. The visual description of the flow is explained in Section 4. Section 5 describes the experimental results and their comparisons with the analytical model.

2. Physical model

There is a considerable amount of literature upon single droplet evaporation model in the combustion research field (W.A. Sirignano [9]). The aim of the present study is to choose a relatively simple approach (1D) reproducing the general trend of the measurements. Following the derivation of H. Pretrel [10], a first order differential equations system is solved with MathCAD 2001 Professional (©1986-2000 MathSoft, Inc.). The system may be presented in a reduced form as a set of four equations:

$$\frac{du_p}{dt}=\frac{u_g-u_p}{\tau};\quad \frac{dT_p}{dt}=\frac{T_g-T_p}{\tau_t}-\frac{Lh_p}{Cp_p}\frac{1}{\tau_m};\quad \frac{d\Phi_p}{dt}=\frac{-\Phi_p}{3\tau_m};\quad \frac{dx_p}{dt}=u_p \qquad \text{Eq. 1}$$

where the l.h.s. parts are formed by the time derivatives of the four main variables associated with the particle phase (velocity u, temperature T, diameter Φ and distance to the nozzle x). The r.h.s parts contain three relaxation times (τ,τ_t,τ_m, respectively the dynamical, thermal and mass transfer relaxation time of the particle) and the ratio of latent heat-to-heat capacity of the particle in liquid state (Lh/Cp).Throughout this section, extra indices as $_g$ stand for gas properties and $_p$ for particle (a droplet of R134-A in the present case). The definitions of the relaxation times are:

$$\tau=\frac{4}{3}\frac{\rho_p}{\mu_g}\frac{\Phi^2}{C_D\,\mathrm{Re}_p};\quad \tau_t=\frac{1}{6}\rho_p\frac{Cp_p}{k_g}\frac{\Phi^2}{Nu_p};\quad \tau_m=\frac{1}{6}\frac{\rho_p}{\rho_g}\frac{1}{D_{p\to g}\left(y_{p,g}-y_{p,g\infty}\right)}\frac{\Phi^2}{Sh_p} \qquad \text{Eq. 2}$$

where the extra variables are: ρ (volumetric mass), μ (dynamical viscosity), k (conductivity), $D_{p\to g}$ (Mass diffusivity of R134A in air), $y_{p,g}$ (mass fraction of R134-A in gas close to the particle) and $y_{p,g\infty}$ (mass fraction of R134-A in gas at an infinite distance from the particle). A more precise definition of this mass fraction is [12]:

$$y_{p,g} = \frac{M_{R134A} P_{sat}(T_p)}{M_{R134A} P_{sat}(T_p) + M_{AIR}\left(P_{ATMOS} - P_{sat}(T_p)\right)} \qquad \text{Eq. 3}$$

with M for molar mass. To avoid singularity troubles, the value of the mass fraction is limited to be always strictly under unity (the case when temperature of R134A is above boiling temperature). Two different values for the mass fraction at "infinite" distance will be investigated ($y_{p,g\infty} = 0$ & $y_{p,g\infty} = 0.2$). The interface of the droplet is supposed to be at constant temperature (i.e. no internal convection inside the liquid droplet) and at constant saturated vapour pressure for this temperature. This vapour pressure at the surface of the particle may have a higher value than the ambient atmospheric pressure.

In the set of equations in (Eq.2), four dimensionless numbers appear (i.e. $C_D, \mathrm{Re}_p, Nu_p, Sh_p$). They represent respectively, the drag coefficient, the Reynolds, Nusselt and Sherwood numbers associated to the particle. The particle Reynolds number is defined as $\mathrm{Re}_p = |u_g - u_p| \rho_g \Phi_p / \mu_g$. The other numbers rely on a set of correlations based on $\mathrm{Re_p}$. In the present model a drag coefficient correlation is chosen that is also valid out of the Stokes regime (i.e. when $\mathrm{Re_p}>1$) with $C_D = 24\left(1 + 0.2\,\mathrm{Re}_p^{0.63}\right)/\mathrm{Re}_p$. Following the advice of Bussmann & Renksizbulut [11], the correction factor, which is generally used in combustion of solid particles, and known as the "Renksizbulut-Yuen correlation", is not applied here, because according to [11], the Renksizbulut-Yuen's correlation is misused in the case of a highly evaporative particle and in the present study, a superheated liquid particle is under a rapid convective evaporation. The Nusselt and Sherwood correlations are the ones used also by Abramzon & Sirignano [12] written in a form valid out of the Stokes regime:

$$\begin{cases} Nu_p = 2 + \left(\left(1 + \left(1 + \mathrm{Pr}_p\,\mathrm{Re}_p\right)^{1/3}\right)\mathrm{Re}_p^{0.077} - 2\right)/FT \\ Sh_p = 2 + \left(\left(1 + \left(1 + Sc_p\,\mathrm{Re}_p\right)^{1/3}\right)\mathrm{Re}_p^{0.077} - 2\right)/FM \end{cases} \qquad \text{Eq. 4}$$

In the Stokes regime, $\mathrm{Re}_p^{0.077}$ is replaced by one. In Eq. 4, Pr_p and Sc_p are the Prandtl and Schmidt number of the particle. FT and FM are the correction factors taking into account the increased fluxes (compared to Fick diffusion) due to the blowing effect (Stefan fluxes). These correction numbers are expressed in terms of the Spalding factors BT & BM [12] defined as: $FT = \ln(1+BT)(1+BT)^{0.7}/BT$ and $FM = \ln(1+BM)(1+BM)^{0.7}/BM$ with $BT = Cp_p|T_p - T_g|/Lh_p$ and $BM = (y_{p,g} - y_{p,g\infty})/(1 - y_{p,g})$.

The vapour or gas properties used inside of all the correlations are established with a mass averaged formulation at a given mixing temperature (i.e. film temperature of Yuen and Chen see [12]). The Prandtl and Schmidt numbers are built on these mixed properties. For the thermo-dynamical properties of R134-A, data are extracted from Poling et al. [13] and/or the NIST web database. Our approach does not consider the internal flow inside of the droplet as it has been proposed in [12]. The present authors are aware that such a simplification may be more adapted for a solid particle. The set of pde's (1) is solved numerically with a Runge-Kutta solver using variable time step. However, the constant time step solver, which is a RK4, has been also used and no noticeable change in the solution has been found with it.

3. Experimental apparatus and procedure

3.1. Test facility

Fig. 1 shows the experimental installation, which allows the pressurization of liquid R134-A under different pressure values. The pressurized liquefied R134-A is stored at a pressure above its vapour pressure at the ambient temperature (i.e. 6.6 bars at 25°C). Nitrogen gas is introduced into the R134-A tank to control the driving pressure. A pressure transducer monitors the pressure history in the tube connecting the R134A and N2 tanks. At the connection with the R134-A tank, a two-entrance valve allows pressurization with N2 (in) and flow of R134-A (out) simultaneously. The liquid R134-A flows from the tank through a horizontal tube. At the end of this tube, a pneumatic ball valve system is installed and it is operated using pressurized air. A thermocouple is introduced in the tube to measure the temperature of the liquid R134-A before the exposure to the ambient. Different nozzle geometries can be mounted on the pneumatic valve. In the downstream direction of the pneumatic ball valve, a rack of ten thermocouples, which are separated from each other by five centimeters, is mounted.

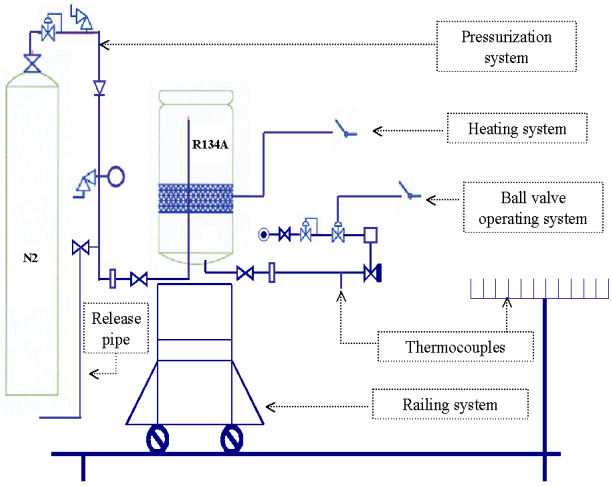

Fig. 1 The experimental facility

3.2. Measurement campaign

The thermodynamical non-equilibrium nature of the flow creates difficulties to obtain accurate data measurements (rapid change in diameter of droplet associated with rapid change in temperature). In the present study, both intrusive and non-intrusive techniques are used to investigate the thermal behaviour of the flashing jet.

For the intrusive technique (rack of thermocouples), the position of the first probe triggers the position of the so-called “flashing point” if this does not occur right at the nozzle exit. After this bursting point, the jet is totally disintegrated and an evaporating spray is observed. Nevertheless, present authors underline that without the triggering probe the position of the flashing point is case dependent and is highly sensible to the superheat level, pressure undershoot, depressurisation rate and nozzle geometry [3,4,5,6,7]. Moreover, measurements presented here are obtained for different distances between the first probe and the nozzle exit in order to observe whether the trend of the measured temperature was sensible to the modulation of the rack distance to the nozzle. A rack of 10 thermocouples with a distance of

0.05m between each other was used in order to observe the axial temperature change at 10 different points simultaneously using a DAS16 acquisition system.

The thermocouples give point measurements in the disintegrated part of the jet. However, information related to the temperature evolution of the unbroken part of the flow (if it exists) between the nozzle orifice and the first thermocouple is not obtained. To obtain thermal information on the upstream portion of the liquid jet, non-intrusive Infrared Camera Thermography measurements are performed using a FLIR Systems' ThermaCAM^{TM} SC3000 camera. It consists of a rugged IR-camera (IP54 housing) with a built-in 20° lens, a remote control, cables and connectors and a range of optical hardware and software accessories. Due to the difficulties of calibrating the camera system with R134-A and difficulty of determining the emissivity of an evaporating mixture of liquid core and aerosols, the obtained thermographs give mainly qualitative information.

4. Visual description of the flow

The Fig. 2 gives the behaviour of the flow under a driving pressure of 7 bars with different nozzle diameters. As it can be concluded from the images, the jet passing through 1 & 2 mm nozzles do have an unstable behaviour since the jet disintegration occurs downstream the nozzle in an unpredictable flashing point whereas for the 4 mm nozzle, the droplet formation occurs right at the nozzle. On Fig. 3, the thermocouples appear as vertical white objects and their impact on the pattern of the flow is obvious (i.e. for the nozzle diameters 1 & 2mm, the first probe is introducing the break-up and droplet formation). In this image, the rack of thermocouples is kept at the same axial distance from the nozzle in all the cases.

5. Results and discussions

5.1. Infrared camera results

Fig. 4 displays a typical thermograph where the liquid core and the first thermocouple placed on the centreline of the jet can be seen. The thermograph values obtained from this figure are scaled to match the temperature value measured by the first thermocouple of the rack. Fig. 5 displays the scaled infrared measurement points extracted from **Fig. 4** along the axial line labelled LO1. It can be observed that the temperature measured inside the tube equals the one given by the thermograph near the nozzle exit. The liquid core does exhibit a rapid decrease of its temperature to the boiling temperature in ambient conditions without noticeable presence of droplets.

5.2. Thermocouple results compared with the analytical evaporation model

On Fig. 6, a representation of the temperature evolution along the jet axis is given in a dimensionless distance to the nozzle (scaled by orifice diameter). It can be noticed that the measured temperature exists above the boiling temperature (super-heating conditions) and goes below the boiling temperature ($T_{boiling}$=-26.7°C at 1atm). Far from the nozzle, the temperature reaches a plateau at about -55°C. In this representation, the smaller the diameter of the nozzle, the smaller is the slope of the temperature decay. Nevertheless, in a dimensional representation all the measured temperatures follow a similar trend (see Fig. 7).

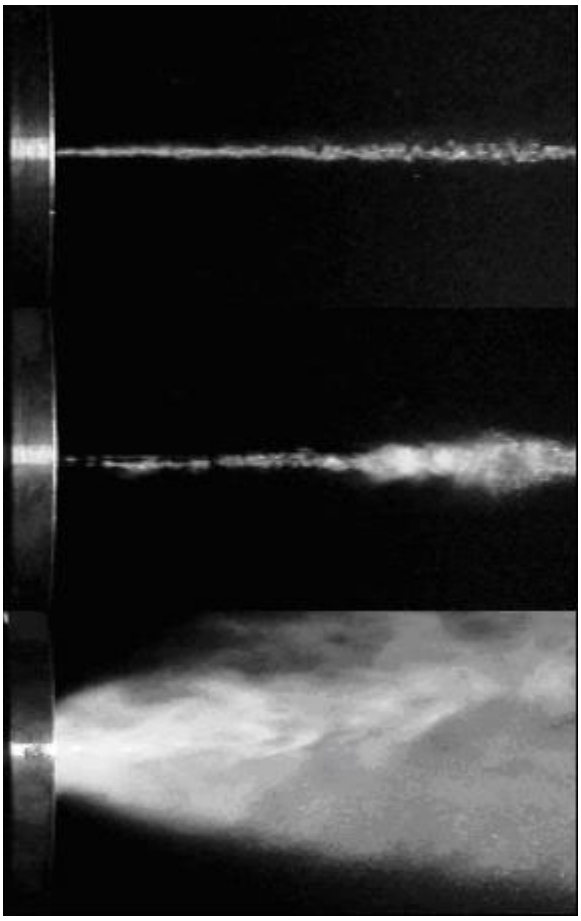

Fig. 2. R134-A jets under 7 bars at 22ºC (Nozzle diameters: 1, 2 and 4 mm from top to bottom)

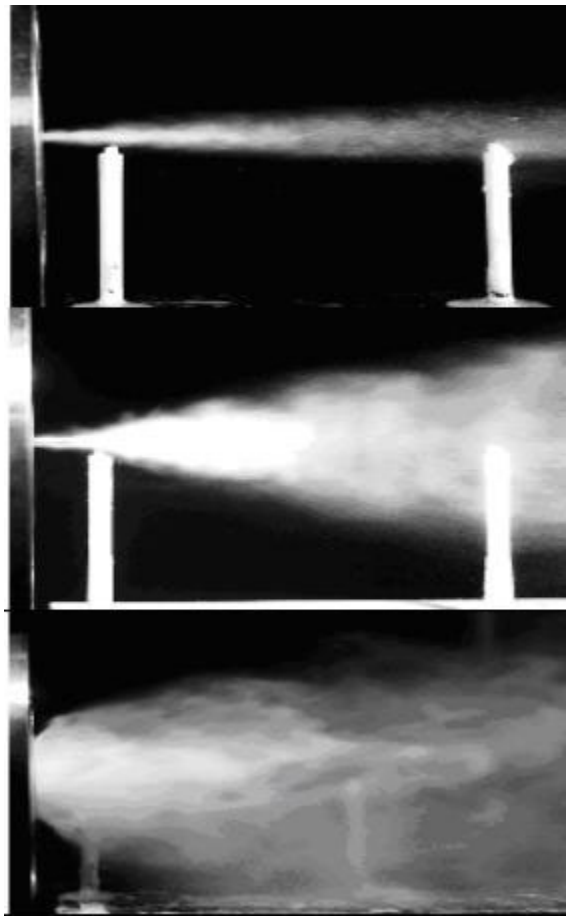

Fig. 3. The first two thermocouples in R134-A jets under 7 bars at 22ºC (Nozzle diameters: 1, 2mm and 4 mm from top to bottom).

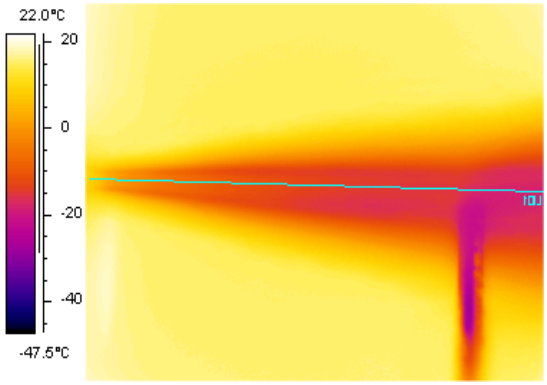

Fig. 4. Infrared thermograph (zoomed image) for the flashing two-phase jet under the pressurization of P=7 bars for the orifice diameter of 1 mm.

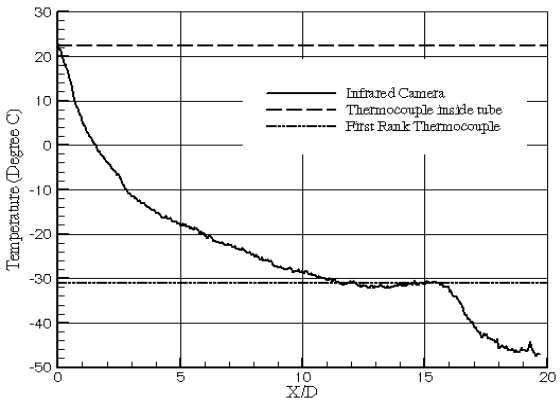

Fig. 5. The temperature profiles of the sections LO1 compared with two thermocouple results on the centreline of the jet (1mm orifice diameter)

The same Fig. 7 displays the comparison between the measurements and the model described in section 2. For the model, some initial values are needed such as: diameter of particles, velocity and temperature (for both particle and surrounding gas), and mass fraction of R134a at infinite distance from the particle. From previous measurement campaigns [1], initial jet velocity has been estimated as 25 m/s with droplet Sauter mean diameter around 200 microns. Air temperature was 25°C at atmospheric pressure, with a gas entrainment arbitrarily fixed at 0.1m/s. The mass fraction of R134-A far from the jet is assumed to take two different values, respectively zero and 20%. Two diameters (200 µm and 300 µm) have been tried in the model.

The temperature associated with the smaller diameter (200 µm) reaches the minimum numerical values quicker (-55°C or -65°C). The results are highly sensitive to the value of mass fraction at infinite distance (respectively 0.2 and 0). It may be seen that the temperature predicted by the simplified model, for both diameters, are following the general trend of measurement points. Nonetheless, some features observed in the experiments are not yet reproduced. For example, air entrainment carried from the exterior of the spray towards its centre, when it is not continuously wetted may heat up the thermocouple (see measurements associated with orifice 4mm on Fig. 7 at 0.6m from the nozzle). It can be noted on Fig. 7 that measurement associated to the smaller orifice diameter exhibits lower temperature values in the near nozzle area, but reaches back the same asymptotic value. This fact could be explained from Fig. 3, where it may be seen that the first thermocouple seems to touch mainly the surface of the jet, producing locally finer droplets and inducing the burst of the jet downstream. It is thought that the difficulty in the alignment of the rack of ten thermocouples with the centreline axis of a jet of 1mm diameter is responsible of this last observation.

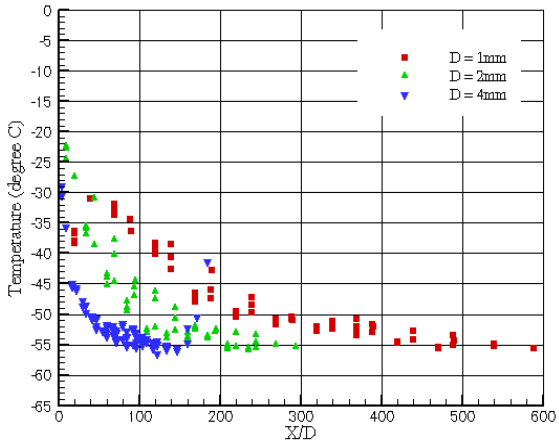

Fig. 6. Measured temperatures for 3 diameters under (initial liquid at 7bars and 22ºC)

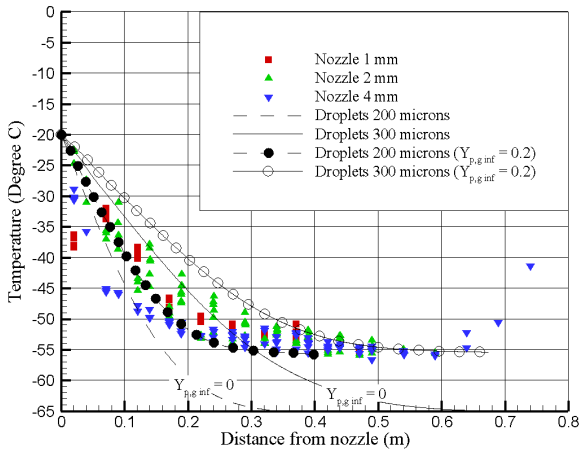

Fig. 7. Comparison between measured temperature and prediction from the model.

6. Conclusions

Intrusive and non-intrusive techniques have been applied to characterize thermally a flashing jet of liquid R134A exiting from a diaphragm type orifice. A simple droplet evaporation model has been used to compare with the measurements. In this approach, improvements are still necessary to correctly describe the rapid evaporation and its relation with ambient air (i.e. convective speed of air, mass fraction at infinite etc). Here, the first measurement probe induced the position of the flashing point for the smaller orifices. It has been observed that

different diameters of orifice may lead to different jet patterns even if the thermocouple measurements do not register a different trend in temperature.

7. Acknowledgements

The authors would like to acknowledge the support of European Commission under the contract number EVG1-2000-22022.

8. References

[1] Yildiz, D.; Theunissen, R.; Van Beeck, J.P.A.J.; Riethmuller, M.L.: "Understanding of dynamics of a two-phase flashing jet using multi-intensity-layer PIV and PDA",11th International Symposium on Application of Laser Techniques to Fluid Mechanics, Lisbon, Portugal, July 8-11, 2002.

[2] Yildiz, D.; Van Beeck, J.P.A.J.; Riethmuller, M.L.: "Global rainbow thermometry applied to a flashing two-phase R134-A Jet",11th International Symposium on Application of Laser Techniques to Fluid Mechanics, Lisbon, Portugal, July 8-11, 2002

[3] Bartak, J.,1990, A study on rapid depressurisation of hot water and the dynamics of vapour bubble generation in superheated water, Int. J. Multiphase Flow, Vol.16, No.5, pp. 789-798.

[4] Brown, R. & York, J.L. 1962, *Sprays formed by flashing liquid jets*, AIChE Jl 8, 149-153.

[5] Elias,E., Chambre, P.L.,1993, *Flashing inception in water during rapid decompression*, Trans. of ASME, J.of Heat Transfer, Vol.115, pp.231-238.

[6] Peter, E.M., Takimoto, A.& Hayashi, Y., 1994, *Flashing and shattering phenomena of superheated liquid jets.* JSME Int. Journl., Series B, Vol 37, No 2, May 1994, pp 313-321.

[7] Peter, E.M, Takimoto, A. & Hayashi, Y., 1995, *Experimental investigation of the mode of phase dissociation in superheated liquid jets*, Int. J. Heat Mass Transfer, Vol.38, No.8, pp 1457-1466

[8] Owen, I., Jalil, J.M., 1991, Heterogeneous flashing in water drops. Int.J. Multiphase Flow, Vol. 17, No 5, pp 653-660.

[9] Sirignano W.A. "Fluid dynamics and transport of droplets and sprays" Cambridge University Press 1999

[10] Pretrel H. " Etude du comportement thermohydraulique de pulvérisations liquides sous l'effet d'un rayonnement infrarouge. Application à la protection incendie par rideau d'eau " Ph. D thesis Institut National des Sciences Appliquées de Lyon (France) 1997

[11] Bussmann M., Renksizbulut M. "Convective Evaporation of an extremely volatile fuel droplet" Technical Notes, J. Thermophysics, Vol. 4, No. 4, October 1990.

[12] Abramzon B., Sirignano W. A. "Droplet vaporization model for spray combustion calculations" Int. J. Heat Mass Transfer Vol.32, No. 9, pp. 1605-1618, 1989.

[13] Poling B.E., Prausnitz J.M. and O'Connell J.P. "The properties of gases and liquids" Fifth Edition, McGraw-Hill 2001.